scientific reports

Check for updates

OPEN

Macular patterns of neuronal and visual field loss in recovered optic neuritis identified by machine learning

David Szanto[1], Jui-Kai Wang[2,3,4], Brian Woods[5], Tobias Elze[6], Mona K. Garvin[2,4], Louis R. Pasquale[7], Randy H. Kardon[2,8], Joseph Branco[9] & Mark J. Kupersmith[1,7]✉

We used machine learning to investigate the residual visual field (VF) deficits and macula retinal ganglion cell (RGC) thickness loss patterns in recovered optic neuritis (ON). We applied archetypal analysis (AA) to 377 same-day pairings of 10-2 VF and optical coherence tomography (OCT) macula images from 93 ON eyes and 70 normal fellow eyes ≥ 90 days after acute ON. We correlated archetype (AT) weights (total weight = 100%) of VFs and total retinal thickness (TRT), inner retinal thickness (IRT), and macular ganglion cell-inner plexiform layer (GCIPL) thickness. AA showed most ON eyes had a 10-2 VF pattern like the normal fellow eye VF, despite having markedly thinner GCIPL patterns. AA identified 7 VF and 11 retinal thickness ATs for each OCT model. The normal VF AT constituted 80% of ON eyes and 90% of normal fellow eyes. The most common GCIPL AT consisted of diffuse thinning. We identified significant correlations for the normal AT weights using OCT AT weights of five GCIPL ATs ($r = 0.45$), four TRT ATs (0.53) and two IRT ATs (0.42). Following acute ON, most eyes had complete 10-2 VF recovery despite significant GCIPL thinning, suggesting compensatory mechanisms for vision.

Optic neuritis (ON) is the most common acute demyelinating optic neuropathy that is typically idiopathic or related to multiple sclerosis (MS)[1]. Despite quite often presenting with severe vision loss, the visual prognosis tends to be good. However, residual visual deficits sometimes remain within the central 30 degrees of visual field (VF) and with contrast sensitivity testing[2,3].

Assessment of the central 10 degrees of the visual field by the 10-2 Humphrey visual test (Zeiss-Meditec, Inc, Dublin, CA) utilizes 2 degree spacing of test locations to provide a much denser sampling of the central VF, which is more sensitive than 24-2 for identifying subtle paracentral VF defects. Studies using 10-2 strategy in glaucoma have revealed central VF loss more frequently than previously suspected[4]. ON almost always initially affects central visual function[5]. Following an episode of acute ON, the frequency of residual loss in the 10-2 VF is similar to having abnormal low contrast visual acuity after an attack[6]. In the setting of MS, even in eyes without a history of ON, visual function can be notably impacted, with delays and asymmetries in pupillary responses observed[7].

Approximately 73% of ON eyes exhibit retinal nerve fiber layer (RNFL) thinning on optical coherence tomography (OCT) following an episode[8–10]. At acute ON onset, the RNFL is often normal or thicker, due to swelling. Ganglion Cell-Inner Plexiform Layer (GCIPL) is normal at presentation and the average is frequently thinner after 1 month[9]. GCIPL thinning occurs in approximately 96% of ON eyes[10]. As the RNFL determination reflects both swelling and axonal thinning or loss, GCIPL thickness is the preferred metric in the detection of neuronal thinning or loss for ON during the first 3 months post presentation[10].

Structure-function relationships have been extensively explored in another optic nerve disorder, glaucoma. Recent studies report abnormalities in the central VF and macula ganglion cell layer[11–13]. Prior work on ON suggests when there is poor recovery of the VF, RNFL thinning correlates with major residual impairment of

[1]Neurology, Icahn School of Medicine at Mount Sinai, New York, USA. [2]Center for the Prevention and Treatment of Visual Loss, Iowa City VA Health System, Iowa City, IA, USA. [3]Department of Ophthalmology and Visual Sciences, University of Iowa, Iowa City, IA, USA. [4]Department of Electrical and Computer Engineering, University of Iowa, Iowa City, IA, USA. [5]Irish Clinical Academic Training Programme, Department of Ophthalmology, Cork University Hospital, Cork, Ireland. [6]Schepens Eye Research Institute, Harvard Medical School, Boston, MA, USA. [7]Ophthalmology, Icahn School of Medicine at Mount Sinai, New York, USA. [8]University of Iowa Carver College of Medicine, Iowa City, IA, USA. [9]New York Medical College, Valhalla, NY, USA. [10]Corresponding Author: ✉email: mark.kupersmith@mountsinai.org

the central 30 degrees of the VF as measured by standard automated perimetry (SAP)[8]. However, as the OCT measured GCIPL thinning is strongly correlated with the 10-2 mean deviation (MD) across all eyes after ON, we hypothesized that ON would cause measurable patterns of structural and functional damage. Study of the residual loss could provide an improved structure-function relationship for ON better than prior VF and OCT RNFL investigation[6].

Archetypal analysis (AA) is a data dimensionality reduction method that has been applied for unsupervised VF analysis[14]. The algorithm identifies extremal points in a dataset, dubbed archetypes (ATs), where each data point can be expressed as a weighted combination of these ATs. Previously, our group utilized AA to show residual quantifiable regional VF deficits in ON when using 24-degree SAP[15]. In this study we explored whether AA could find patterns of residual 10-2 VF loss and structural loss in the corresponding macula after an ON episode. We examined whether patterns of GCIPL and VF loss in the macula correspond after recovery of optic neuritis. AA is a well-recognized method in VF research and was selected over other methodologies such as canonical correlation analysis. Our goal was to identify meaningful patterns of macular thickness and VF changes, rather than simply maximizing the correlation between the two, ensuring the findings are clinically relevant.

To our knowledge, mapping of the 10-2 VF patterns to the macula thickness measurements in ON has not been described previously. We explored whether total retinal thickness (TRT), inner retinal thickness (IRT), or GCIPL thickness correlate with 10-2 VF deficits after ON recovery. We postulated that applying machine learning methods to analyze the 10-2 and OCT GCIPL would reveal clinically relevant patterns of structural and functional loss after an acute ON episode. In a subset of eyes, we also hypothesized that the more severe pattern of thinning of the GCIPL after an acute optic neuritis attack would more strongly correlate with the 10-2 VF patterns of loss and the mean deviation (MD).

Methods

This study was approved by the Institutional Review Board of the Icahn School of Medicine at Mount Sinai. The requirement for informed consent was waived by the Institutional Review Board of the Icahn School of Medicine at Mount Sinai. The datasets generated and/or analyzed during the current study are not publicly available due to containing medical information but are available from the corresponding author on reasonable request. The data for this study was collected in accordance with the tenets of the Declaration of Helsinki.

Data availability

The datasets generated and/or analyzed during the current study are not publicly available due to containing medical information but are available from the corresponding author on reasonable request.

Datasets

We reviewed the records from one neuro-ophthalmology service of all patients with documented ON (excluding other inflammatory optic nerve disorders) that had spectral domain (SD) OCT and 10-2 VF performed at a visit after recovery. ON was diagnosed by the following criteria: acute unilateral vision loss; pain in the eye or pain with eye movement; relative afferent pupillary defect (unless fellow eye had history of ON) and normal funduscopic examination, and no medication or systemic inflammatory disorder that could cause optic nerve injury. At presentation, almost all patients had 1.5 tesla orbital MRI performed with fat suppression, gadolinium T1 weighted and short tau inversion recovery images. We excluded eyes with age-related macular degeneration, epiretinal membrane, glaucoma, other optic neuropathy, any disorder that could cause acquired thinning or thickening of the macula, or inadequate VF and OCT data. We also did not include subjects that were taking drugs that are known to cause vision loss, such as PDE-5 inhibitors, ethambutol, amiodarone, hydroxychloroquine, isoniazid, and linezolid.

We selected subjects that had 10-2 Swedish interactive threshold algorithm for SAP tests and Cirrus SDOCT macula volume scan (Zeiss-Meditec, Inc, Dublin CA, qualifying signal strength ≥ 7) performed on the same day at least 90 days after an acute ON attack in the time interval from 6/7/2013 to 9/13/2022. If meeting our criteria, we also collected the same measurements from the fellow eye. A subset of these eyes having relatively poor visual field recovery (MD $<$ -5 dB) was also analyzed separately.

Of the 151 participants with 10-2 VFs, 83 participants met our inclusion criteria. We collected data from 93 ON eyes and 70 fellow eyes that were considered normal. Although some participants had bilateral ON, each eye was treated as an independent event, as there is no evidence that injury in one eye influences the other at a different time. We selected a follow-up period of greater than three months, as GCIPL loss typically occurs within this timeframe[9,10]. Given the fluctuating nature of ON and its potential for recurrence, follow-up duration was not included in our statistical model. As the data were retrospective from real-world settings, baseline OCT information prior to the attack was unavailable. In the context of MS, we excluded the fellow eye demarcation if there was a history of ON in that eye. The occurrence of other abnormalities outside our exclusion criteria is rare.

While our sub-analysis of VFs with poor recovery was relatively small ($n=25$), we did have a larger number of ON VFs with poor recovery but without accompanying OCT ($n=50$). We trained our VF model on the larger dataset and tested on the smaller one (Table 1). The criteria for having a normal fellow eye included having no retinal or optic disorder, no prior history of ON, an OCT with average RNFL and GCIPL thickness in the manufacturer's normative range, no optic disc pallor, no macula pathology by direct ophthalmoscopy and OCT macula imaging, and no abnormality in that optic nerve by MRI. The normal fellow eye conditions are as exact as feasible to provide a matched control group to ON, as we acknowledge that subclinical ON is possible despite our rigorous criteria.

VF testing was performed by trained technicians with expertise in obtaining VFs that met clinical trial quality control standards. Repeat VFs were performed at each visit if quality parameters were needed and the data from

	Patients	Eyes	Visual fields	Paired with OCT data
Model 1	83	ON: 93 Fellow: 70	ON: 233 Fellow: 144	Yes
Model 2 (training, MD < − 5)	32	ON: 35 Fellow: 0	ON: 50	No
Model 3 (testing, MD < − 5)	17	ON: 18 Fellow: 0	ON: 25	Yes

Table 1. Archetype-derived visual field models. We report the construction of three models describing visual field archetypes of eyes at least 90 days after acute optic neuritis attack. Model 1 encompasses all the data points where visual field information is paired with same-day optical coherence tomography data. Due to the larger number of eyes with poor vision (mean deviation < − 5) but lacking retinal thickness data, we trained archetypes on this specific group of eyes (model 2). Model 3 shares the same visual field archetypes as model 2; however, they are assigned different weights due to their derivation from the decomposition of a smaller dataset that includes both visual field and optical coherence tomography information.

the most reliable VF was used. VFs were deemed unreliable and not included if false positive or negative errors were greater than 30%, or fixation losses exceeded 33%.

OCT segmentation and 10-2 visual field mapping thickness maps

For each of the available OCT macular scans ($6 \times 6\ mm^2$), our 3D graph-based segmentation approach identified the internal limiting membrane (ILM), the boundaries of the ganglion cell plus inner plexiform surfaces, the inner boundary surface of the outer plexiform layer (OPL), and outer surface boundary of the retinal pigment epithelium (RPE) complex[16,17]. Based on the layer segmentation, the GCIPL, the inner retina (IR; from the ILM to OPL, including the bipolar cell layer) and the total retina (TR; from the ILM to RPE) thickness maps were computed. Then, the fovea was automatically detected within the central macular region based on the GCIPL thickness map. The segmentation outcomes, fovea detection, and thickness maps were passed through quality control (by JKW). The OCT scans with inaccurate layer segmentation (due to poor image quality, image motion artifacts, and/or equivocal identification of retinal layers because of severe atrophy) were further excluded; we used a similar data preparation pipeline in previous studies[18].

To correlate the retinal structural measures with the 10-2 VF functional outcomes, the x-y locations of the 10-2 VF 68 points were adjusted to account for the previously described retinal ganglion cell displacement near the fovea[19]. We aligned the thickness maps among all the eyes according to the fovea location. However, because not all the OCT scans were perfectly centered at the fovea, we omitted the two measured points at the extreme superior, nasal, temporal, and inferior poles, resulting in a total of 60 points in the OCT thickness map) to handle the missing information. Of the 22,620 OCT points measured, we could not calculate 10 and we replaced their values with the mean thickness at the missing location.

AT analysis

We used the open-source software module "archetypes" within the Python programming environment to run AA[20]. All VFs and OCTs from the left eye were converted to right-eye format. For each OCT (based on the GCIPL, IR and TR thickness maps) and VF AA model, we used 10-fold cross-validation to select the number of ATs (such that all data was divided into 10 subsets, with each being used as the testing set once, and the others serving as the training set) for each model. Using total deviation (TD) data, we established three VF models: model 1, model 2, and model 3. Model 1 is derived from VFs that contain same day OCT pairings ($n = 233$). Model 2 describes VF ATs of a larger dataset of VFs ($n = 50$) with poor vision (MD < -5) but without OCT data. Model 3 uses model 2 VF ATs but decomposed on a smaller dataset of VFs ($n = 25$) that also includes linked OCT information (Table 1). Some groups have previously unlogged TD measurements (in apostilbs) when conducting structure-function analysis[12]. We chose to present the data by examining the VF in a logarithmic scale (as opposed to transforming it via taking the antilog) as this is more common clinical practice. Additionally, using the logarithmic scale aids in distinguishing between moderate and severe cases of vision loss. By applying AA to un-logged TD measurements there is an overrepresentation of poor vision, underrepresentation of specific patterns related to improvement, as well as the loss of relationships between TDs. Conversely, we considered eyes with MD ≥ -5 as having a good recovery of 10-2 VF. Our three OCT models were constructed using all OCT data associated with visual fields in model 1. We divided each model based on the thickness analyzed, resulting in the TRT model, the IRT model, and the GCIPL model. For each VF and OCT model, we calculated the residual sum of squares (RSS) between our data and the model's reconstruction of the data from two to 20 ATs. We created plots for each model, displaying the relationship between the number of ATs and their corresponding RSS. We utilized the elbow method to identify the optimal number of ATs to minimize RSS and thus prevent overfitting. We normalized the sum of relative weights (RW) of all ATs within each model to sum to 100%. The ATs are ordered by RW (representing frequency within the dataset). We decomposed each VF and OCT into component ATs, such that each was represented by some number of AT weighting coefficients summing to 100%.

Defining threshold value for meaningful weight and weight change

To determine a "clinically meaningful" AT RW we chose a conservative minimum weight value of the reciprocal of the number of ATs (1/k) to ensure that each AT had clinical relevance and to reduce noise due to randomness.

We defined a meaningful RW for the seven-AT-ON VF model to be greater than 1/7 or > 14%, the RW for the sub-analysis 10-AT-ON VF model to be greater than 10%, and the RW for all three 11-AT-ON OCT models to be greater than 9%.

Statistical analyses

We performed all statistical analyses in a Jupyter notebook with Python 3.8.8. All visualizations were done with the open-source python module "matplotlib"[21]. Using model 1, we compared RWs of the same AT across different subsets with a two-sample two tailed t-test for equal means ($\alpha = 0.05$). We used the module "statsmodels" to linearly regress VF measurements (AT weights and MD) and OCT AT weights[22]. We correlated individual meaningful VF measurements using all OCT AT weights with $p < 0.05$, as well as mean GCIPL thickness of all eyes ($n = 93$) in model 1 (Fig. 1). We used Akaike Information Criterion (AIC) to ensure that our model is sufficiently fit. For our main study, we corrected for multiple data comparisons with a false discovery rate cutoff of 5%. In our sub analysis, we did not correct for multiple comparisons since the sample size was small.

Results

We investigated a total of 83 participants (10 of whom had ON in the fellow eye > 90 days after the first eye episode), with a mean age of 44.1 ± 14.2 years (s.d.), and 30% were male. We diagnosed MS in 42% of patients concurrently with ON diagnosis, and 7% of participants had MS prior to ON onset. The median number of days since an ON attack was 1084 days with an interquartile range of 2468 days. At least 90 days after the acute ON attack, the mean MD was −2.38 ± 4.07 dB (s.d.) in the ON eye and −0.52 ± 1.34 dB in the fellow eye (t-test $p < 0.001$). In our sub-analysis study (MD < -5 dB) ON eyes, the average MD was −11.01 ± 6.52 dB. Figure 2 shows the pointwise mean GCIPL thickness plots of all the ON and normal fellow eyes over these 60 points. GCIPL eyes (mean = 68 µm) were markedly thinner in the central ~ 8° in ON eyes (mean = 85 µm, $p < 0.001$), with a more similar but still significant ($p < 0.001$) peripheral thickness between the two (mean = 47 µm and 53 µm, respectively).

We determined that the optimal number of VF ATs was seven in our main study and 10 in our sub-analysis of patients with poor average VF recovery (Fig. 3). We selected 11 as the optimal number of OCT ATs for all categories of retinal thickness (Fig. 3, Supplemental Fig. S1).

10-2 VFs decomposed into model 1

Model 1, the seven-AT VF model (Fig. 4) created from 10-2 VFs of ON eyes showed a range of patterns, ordered by their RW, or frequency of occurrence. AT1, which approximates a normal VF, was the most common VF pattern with a RW of 80%. The remaining six ATs all had RW < 6%. For eyes with good recovery (MD ≥ -5

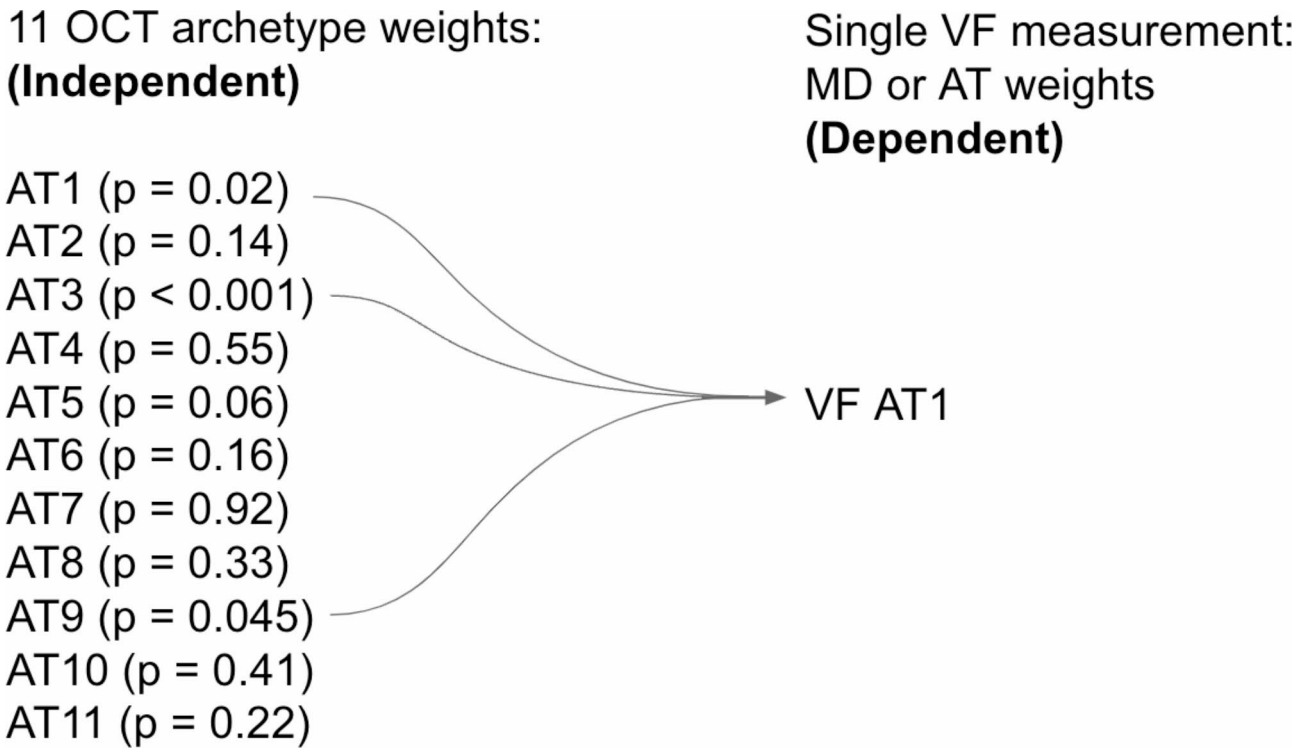

Fig. 1. Linear regression of a single VF measurement using OCT archetypes. Linear regression analysis between the weights of 11 optical coherence tomography archetypes as the independent variable and a single visual field parameter (such as Mean Deviation or visual field archetype weight) as the dependent variable. Only the variables with weights $p < 0.05$ are included in the analysis.

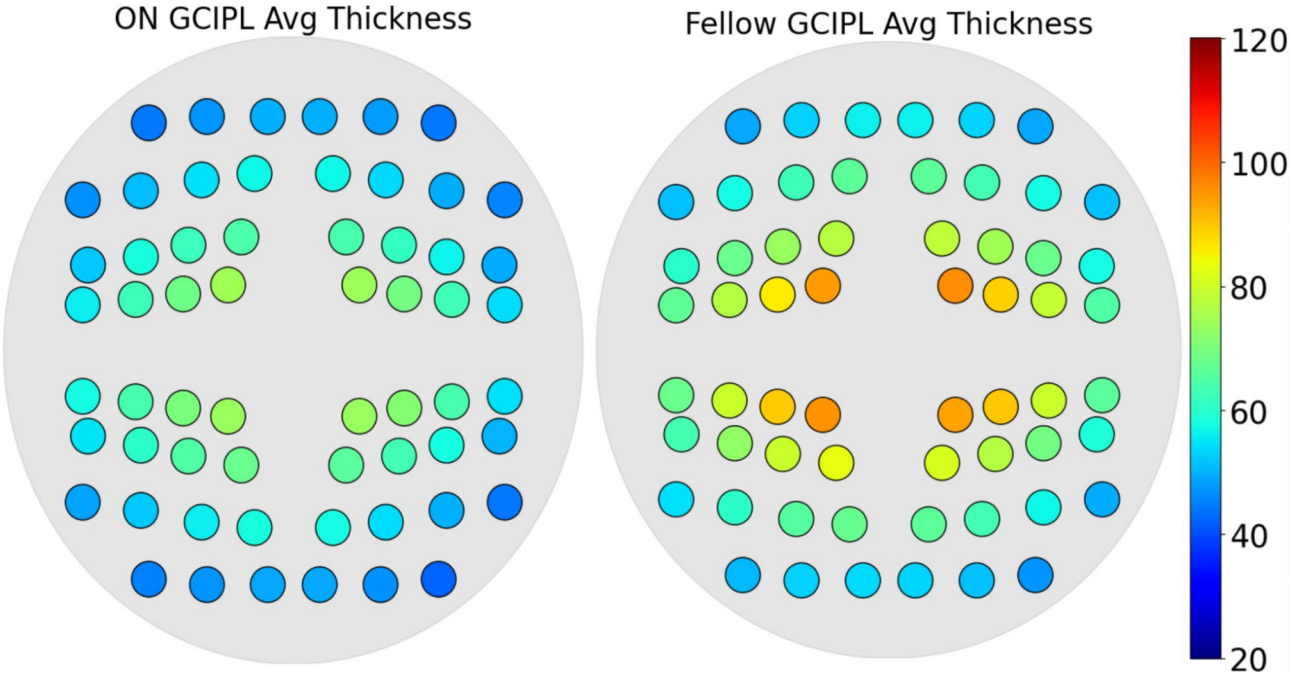

Fig. 2. GCIPL pointwise average of all ON and fellow eyes. Ganglion cell-inner plexiform layer thicknesses (μm) for all optic neuritis eyes (left) and the normal fellow eye (right). While the peripheral thickness is similar, there was marked central thinning in optic neuritis eyes.

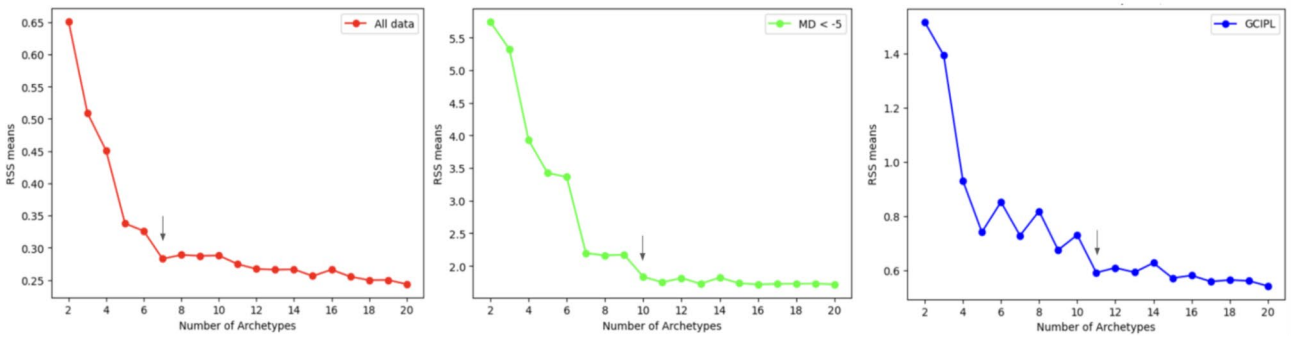

Fig. 3. Residual sum of squares. Residual sum of squares plot for determining the optimal number of archetypes for visual fields and optical coherence tomography. We determined the optimal number of archetypes as seven for all data, 10 for visual fields with mean deviation < -5 dB, and 11 for optical coherence tomography for the ganglion cell-inner plexiform layer, denoted by the arrows. This is the point where the curve flattens where the model also shows distinct visual field archetypes, ensuring their predictive abilities without overfitting.

dB), using the ATs derived from model 1, decomposition of this subset showed an AT1 RW of 85.4% (95% CI 0.84–0.87). Among normal fellow eyes decomposed using model 1 ATs, we find that AT1 had a RW of 90.2% (95% CI 0.89–0.91). While significantly different ($p < 0.002$), the RW is close in value. We also generated a separate model with all normal fellow eyes meeting our inclusion criteria, where the patterns and average TDs were mostly similar and normal, indicating overall normal VFs (Supplemental Fig. S2).

OCT AT model for TRT, IRT, and GCIPL

Using the criteria defined in the "Methods" section, the 11-AT OCT TRT, IRT and GCIPL models yielded more meaningful ATs than the AA model for VFs. The GCIPL AT model found four meaningful (RW ≥ 9.1%) ATs (Fig. 5). For the GCIPL model, the thinner AT1 had a RW of 21% (95% CI 0.18–0.24) in ON eyes and a RW of 0.5% (95% CI 0.00–0.01) for fellow eyes ($p < 0.001$). In contrast, the thicker GCIPL AT3 was better represented in fellow eyes with a RW of 28% (95% CI 0.24–0.32) than in ON eyes ($p < 0.001$) with a RW of 13% (0.10–0.15).

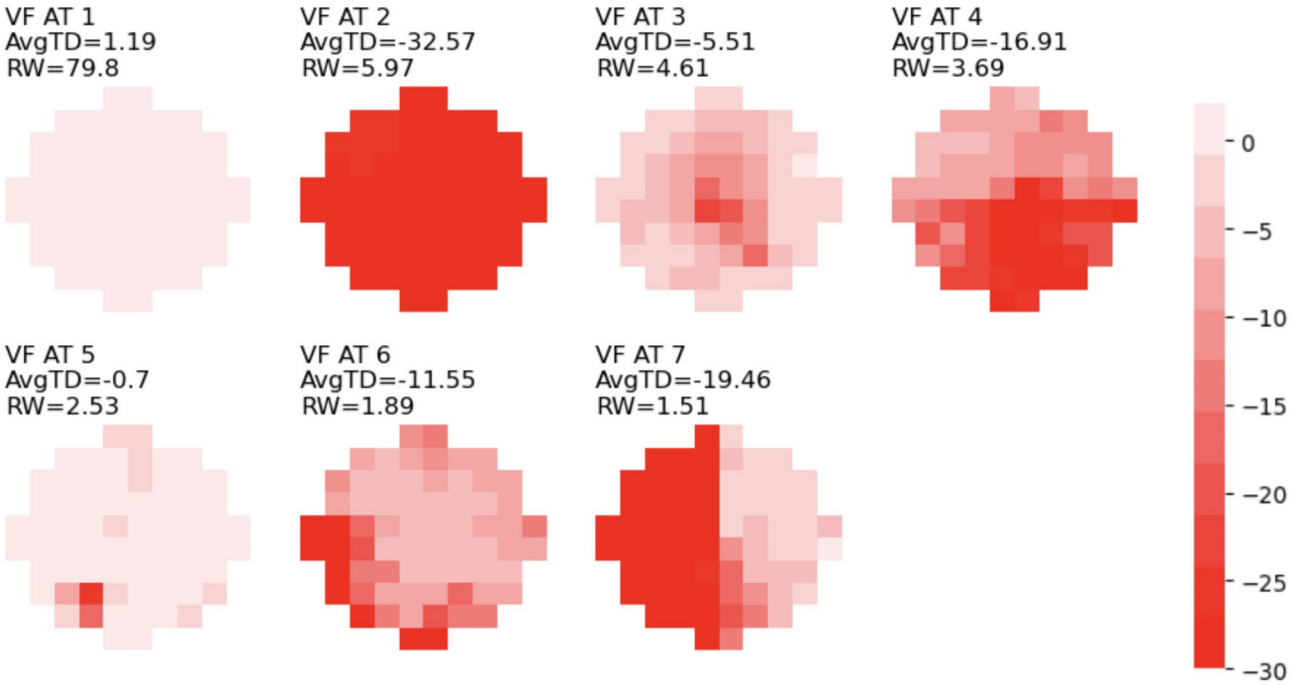

Fig. 4. Seven 10-2 VF ON archetypes. Visual fields of model 1. The varying shades of red within each archetype denote total deviation values, and scale at the right denotes the total deviation values associated with each shade. The color scales range from − 30 dB to 0 dB. Each archetype is shown along with its corresponding average total deviation value and relative weight (shown as percentage) within the dataset. The archetypes are numbered and displayed in order of relative weight.

GCIPL, IRT and TRT AT correlation with 10-2 VF parameters

In a linear regression correlating a single VF variable (meaningful AT or MD) with significant ($p<0.05$) OCT AT RW coefficients across all three OCT models, we found a significant correlation with OCT AT RWs for GCIPL AT2, AT3, AT4, AT5, AT8, and AT11 with MD ($r=0.67$). For TRT, AT1, AT3, AT5, AT11 RWs were best correlated with VF AT1 ($r=0.53$) (Table 2). IRT ATs had a weaker correlation with both MD ($r=0.56$) and VF AT1 ($r=0.42$). The average GCIPL thickness correlated only modestly with MD and the VF AT1 RW ($r=0.37$ and $r=0.41$), and this regression had a higher AIC when compared to our AT models, indicating a lower quality model. A positive correlation coefficient indicates a positive linear relationship between OCT ATs and VF ATs/MD.

Sub-analysis of patients with poor recovery of visual field (MD < − 5 dB)

AA identified three meaningful patterns of VF loss after a sub-analysis of these eyes. Figure 6 demonstrates that model 3, the 10 poorly recovered VF AT model, identified ATs with diffuse moderate VF loss (RW 26%), diffuse major vision loss (RW 15%), and major central 2° with moderate peripheral vision loss (RW 14%). Most data points were composed of VF ATs 1–3 (Fig. 7). We found OCT AT RWs had higher correlation with VF AT RWs when the recovery of the VF was relatively poor. GCIPL ATs best correlated with all meaningful poorly recovered VF AT RWs and MD in model 3 (Table 3). In most cases for TRT and IRT, there were no OCT ATs that correlated by linear regression with relevant VF measurements. Table 3 shows GCIPL AT1 ($p=0.006$) and AT4 RWs ($p<0.001$) strongly correlate with MD ($r=0.78$) via linear regression. The diffuse moderate VF AT1 RW is well correlated ($r=0.65$) with GCIPL AT1 ($p=0.009$), AT4 ($p=0.04$), and AT10 ($p=0.03$) RWs. The diffuse major VF AT2 RW is strongly associated ($r=0.91$) with GCIPL AT 1 ($p=0.003$), AT 4 ($p<0.001$), AT 5 ($p=0.002$), and AT 6 ($p=0.02$) RWs. The mean GCIPL thickness is a poor correlate with relevant VF measurements (r range 0.11–0.28). Lastly, the major central 2° with moderate peripheral vision loss VF AT3 RW is somewhat associated ($r=-0.40$) with GCIPL AT 5 ($p=0.049$) RW. For eyes described by model 3, the RW of GCIPL AT1 (a thinner AT) increased to 28% while the RW of thick ATs AT3, AT4, and AT5 significantly decreased (Table 4).

Discussion

This study demonstrated that AA identifies ON-specific patterns of central 10-degree VF loss primarily when vision is severely affected and can accurately reveal patterns of macular retinal thickness, particularly following an episode. We were surprised that AA did not show more eyes with definitive 10-2 residual losses, focal or diffuse, despite marked thinning of the macula GCIPL. Macula TRT and IRT, utilized to overcome potential sampling problems from GCIPL thinning, did not provide data beyond what was identified using the 3D segmented GCIPL. Since different GCIPL thicknesses and patterns corresponded to a similar VF, we found GCIPL AT

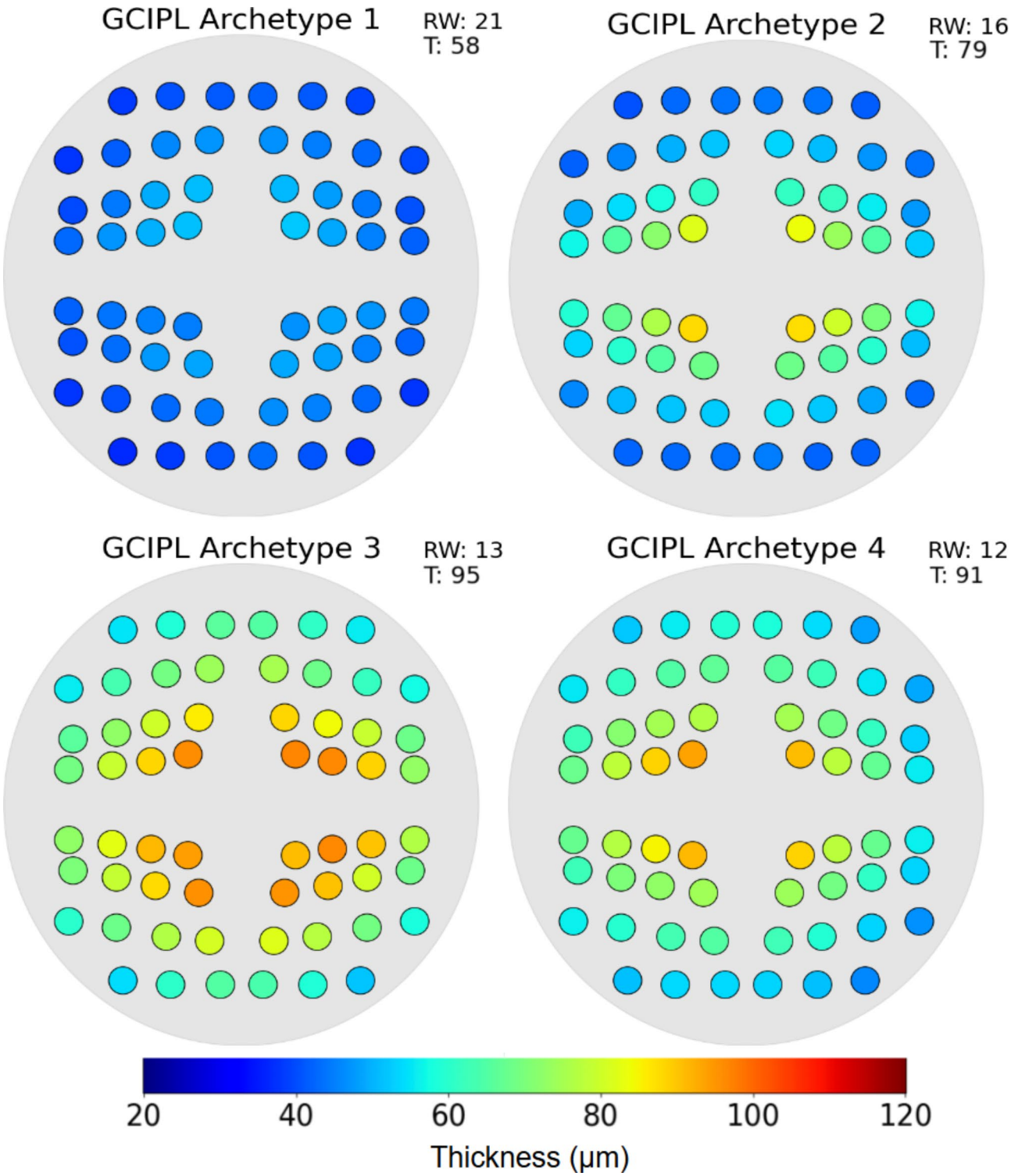

Fig. 5. Four meaningful GCIPL ATs. The gray circle bounds the macula (6×6 mm^2), and the colors correspond to the point thickness at the specified location, along with relative weight and average thickness. Ganglion cell-inner plexiform layer AT1 was markedly thinner than the other archetypes at all points, and AT3 was the thickest archetype, especially in the central four points.

weights only moderately corresponded to the normal VF AT weight. For eyes with poor visual field recovery, AA found three distinct patterns of VF loss that were well correlated with GCIPL ATs. The mean GCIPL thickness at outcome, a global measurement showed the weakest correlation with all of the outcome VF AT values.

Most eyes with ON recovered to a normal central visual field, reaffirming the findings of Optic Neuritis Treatment Trial, which used the $30-2$ strategy[3]. There was a minimal, but statistically significant, difference

	TRT	IRT	GCIPL	Mean GCIPL thickness
MD	$r=0.44$ AIC = 1260 AT1-$p=0.002$ AT5-$p<0.001$ AT7-$p=0.02$ AT8-$p=0.02$	$r=0.56$ AIC = 1229 AT5-$p<0.001$ AT10-$p<0.001$	$r=0.67$ AIC = 1175 AT2-$p<0.001$ AT3-$p=0.005$ AT4-$p<0.001$ AT5-$p<0.001$ AT8-$p<0.001$ AT11-$p<0.001$	$r=0.37$ AIC = 1280
VF AT1	$r=0.53$ AIC = − 129 AT1-$p=0.006$ AT3-$p<0.001$ AT5-$p<0.001$ AT11-$p<0.001$	$r=0.42$ AIC = − 105 AT5-$p<0.001$ AT10-$p<0.001$	$r=0.45$ AIC = − 116 AT2-$p=0.004$ AT3-$p=0.007$ AT4-$p=0.005$ AT8-$p<0.001$ AT11-$p<0.001$	$r=0.41$ AIC = − 106

Table 2. OCT ATs by thickness regressed with individual VF measurements. We report significant optical coherence tomography meaningful archetypes for each thickness subtype and mean ganglion cell-inner plexiform layer thickness correlation with either mean deviation or visual field AT1. We omitted all visual field archetypes that did not have a meaningful relative weight. As indicated by the Akaike Information Criterion and r-value, ganglion cell-inner plexiform layer correlated better than inner retinal thickness and total retinal thickness for mean deviation, and total retinal thickness was best associated with visual field AT1. Average ganglion cell-inner plexiform layer thickness was least predictive among all categories.

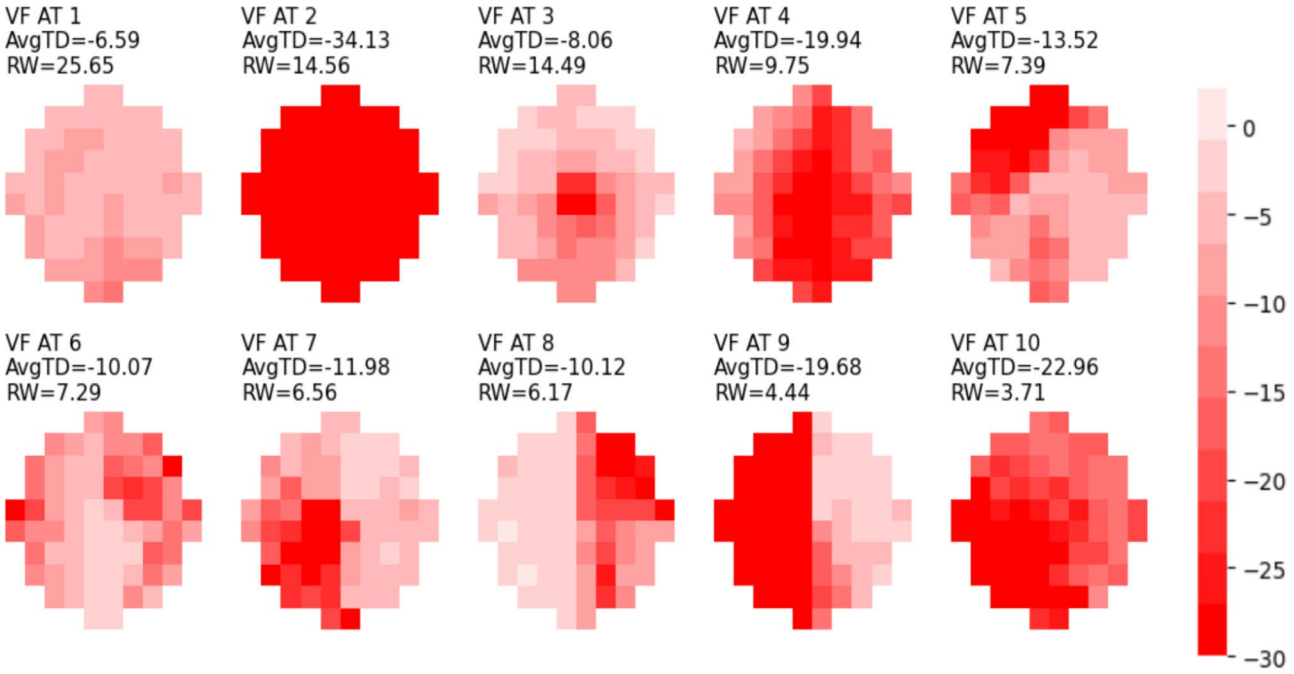

Fig. 6. Ten poor vision 10-2 VF ON archetypes. Visual fields of model 3, containing archetypes of optic neuritis eyes with deficient visual fields (mean deviation < − 5), with corresponding average total deviation and relative weight values (shown as percentage). The varying shades of red within each archetype denote total deviation values, and scale at the right denotes the total deviation values associated with each shade. The color scales range from − 30 dB to 0 dB. Each archetype is shown along with its corresponding average total deviation value and relative weight within the dataset. The archetypes are numbered and displayed in order of relative weight.

in the makeup of the normal VF AT1 between eyes that recover and fellow normal eyes. Despite similarity in VFs, we found that there is a significant difference in GCIPL thickness between the two groups. ON eyes had significantly thinner GCIPL as illustrated by the percent makeup of GCIPL AT 1, compared with normal fellow eyes, as well as by the decrease in the average thickness values.

We also found that in recovered eyes, even for those with a similar VF pattern, there is a wide range of retinal thickness. This likely contributed to why there was only a modest correlation with VF AT1 weight and GCIPL AT weights, and with TRT AT weights. GCIPL thinning may not be the sole determinant of 10-2 VF patterns in recovered vision. There is evidence that MD remains relatively stable even as retinal ganglion cell

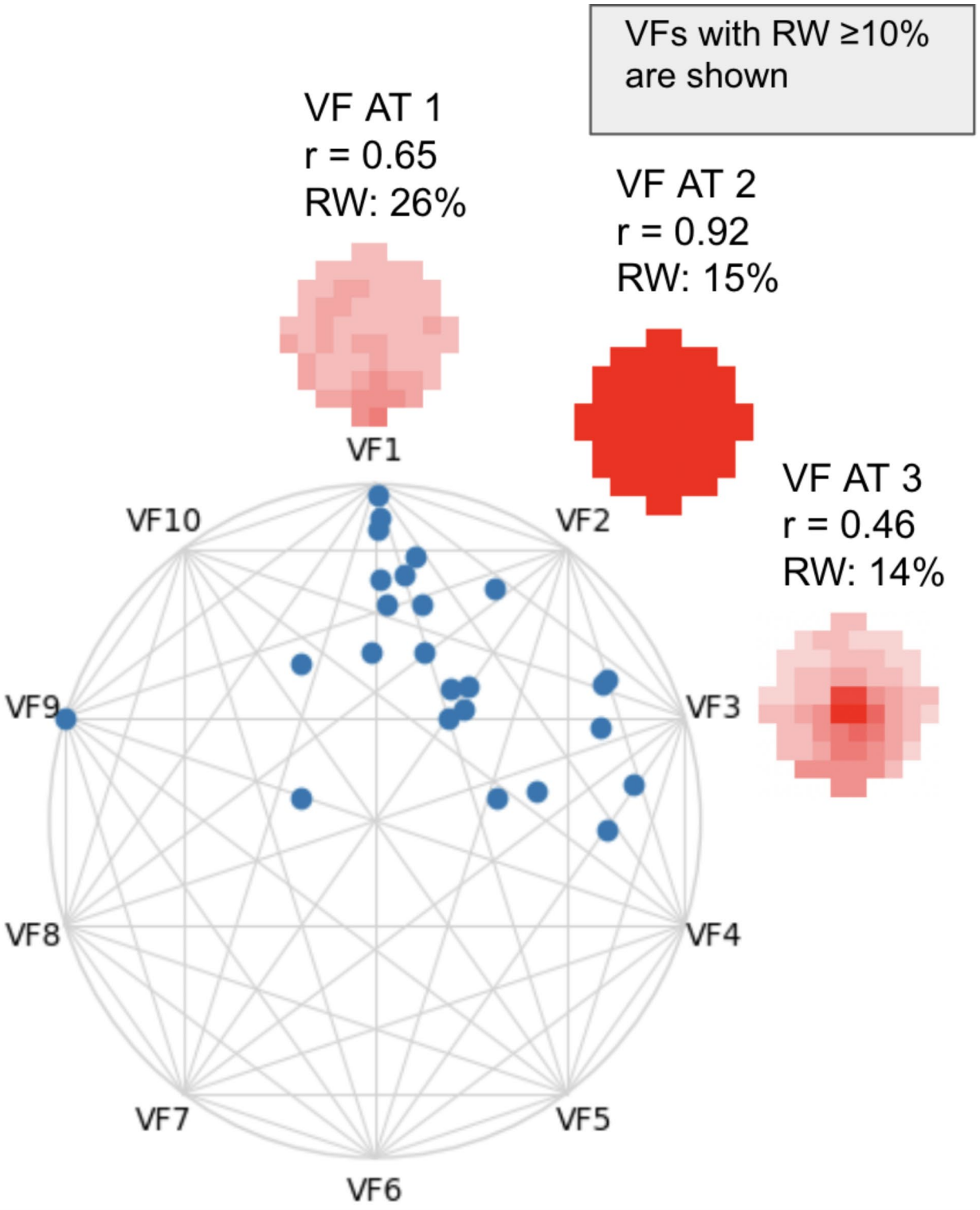

Fig. 7. Simplex plot of deficient visual fields. The three meaningful archetypes from model 3 for eyes with mean deviation < − 5 dB at 90 days or later are shown and the linear regression of all optical coherence tomography ganglion cell-inner plexiform layer archetypes correlated with the three visual field archetypes. Archetypal analysis was trained on deficient outcome visual fields ($n = 50$) and transformed visual fields with same-day OCT pairings ($n = 25$) showing archetype decompositions.

	TRT	IRT	GCIPL	Mean GCIPL thickness
MD		$r=0.52$ AIC = 161 AT4-$p=0.008$	$r=0.78$ AIC = 150 AT1-$p=0.006$ AT4-$p<0.001$	$r=0.11$ AIC = 168
VF AT1	$r=0.45$ AIC = 13 AT4-$p=0.024$		$r=0.65$ AIC = 5 AT1-$p=0.009$ AT4-$p=0.04$ AT10-$p=0.03$	$r=0.22$ AIC = 18
VF AT2		$r=0.61$ AIC = − 28 AT4-$p=0.001$	$r=0.91$ AIC = − 54 AT1-$p=0.003$ AT4-$p<0.001$ AT5-$p=0.002$ AT6-$p=0.02$	$r=0.14$ AIC = − 17
VF AT3			$r=-0.40$ AIC = − 12 AT5-$p=0.049$	$r=0.28$ AIC = − 10

Table 3. OCT ATs by thickness regressed with individual meaningful VF measurements for THOSE WITH POOR VISION. For eyes with visual field mean deviation < -5 dB at 90 days or longer, we used significant optical coherence tomography archetypes ($p<0.05$) for each thickness subtype and mean ganglion cell-inner plexiform layer thickness to correlate with mean deviation, visual field AT1, AT2, and AT3. Blank indicates no optical coherence tomography archetypes significantly correlated with that visual field archetype. We omitted all visual field ATs that did not have a meaningful relative weight. As indicated by the Akaike Information Criterion and R-value, ganglion cell-inner plexiform layer correlated better than total retinal thickness or inner retinal thickness for all visual field measurements. The average thickness of the ganglion cell-inner plexiform layer performed markedly worse than its archetypes.

	Overall mean RW (95% CI) Fellow eye VFs: $n=144$ ON eye VFs: $n=233$	MD < − 5 dB mean RW (95% CI) ON eye VFs: $n=25$
GCIPL AT1	Fellow eye: 0.005 [0.0, 0.009] ON eye: 0.21 [0.178, 0.24]	ON eye: 0.28 [0.178, 0.39]
GCIPL AT2	Fellow eye: 0.21 [0.171, 0.249] ON eye: 0.16 [0.136, 0.193]	ON eye: 0.10 [0.026, 0.181]
GCIPL AT3	Fellow eye: 0.28 [0.244, 0.316] ON eye: 0.13 [0.104, 0.148]	ON eye: 0.04 [0.015, 0.069]
GCIPL AT4	Fellow eye: 0.096 [0.071, 0.12] ON eye: 0.12 [0.0098, 0.147]	ON eye: 0.03 [0, 0.057]
GCIPL AT5	Fellow eye: 0.24 [0.215, 0.269] ON eye: 0.09 [0.067, 0.111]	ON eye: 0.02 [0, 0.04]

Table 4. GCIPL AT decomposition for all ON eyes and eyes with poor recovery. Optic neuritis and normal fellow eye ganglion cell-inner plexiform layer decomposition relative weights for all archetypes with relative weight above 9.1% (1/11) compared to the decomposition for these archetype relative weights for optic neuritis eyes where vision is poor, with 95% confidence interval shown. There was a significant difference between optic neuritis and fellow eyes for the thinner AT1 ($p<0.001$), and thicker AT3 ($p<0.001$) and AT5 ($p<0.001$). The relative weight of AT1 increased among eyes with poor recovery, and decreased for AT2, AT3, AT4, and AT5.

loss advances, suggesting higher visual processing centers may mitigate functional impact despite structural changes[23]. Potential compensation could also arise from overlapping or expanded receptor fields[24].

The sub study showed that GCIPL ATs were best associated with VF AT2, a measure of diffuse loss and the MD in eyes with poor visual recovery. Unsurprisingly, the thinned GCIPL AT1 was an important pattern associated with overall visual field loss. Since we can moderately correlate visual field parameters with GCIPL when vision is good, but we correlate poor vision much better, there may be reduction in a critical density of GCIPL through atrophy or neuronal loss that causes a detectable impact on 10-2 VF testing.

In glaucoma, AA appears to be a robust tool to determine structure-function relationships, particularly as damage tends to be more focal early on[25]. In contrast, in acute ON, there is acute diffuse retrobulbar inflammation and edema with associated diffuse vision loss in most cases. And, unlike glaucoma these pathological mechanisms resolve and repair and some degree of remyelination occur over weeks to months. As almost all regions of the retrobulbar optic nerve are affected, the acute injury commonly leads to diffuse thinning of the macula region GCIPL, and fewer eyes with focal GCIPL loss. Alternatively, while there may be more focal areas of GCIPL loss after ON, given its magnitude, our instruments or methods may not detect subtle differences or patterns of focal thinning.

Our study had limitations typical of retrospective analyses. The dataset was relatively small, with 377 VF-OCT pairings. The sub study of ON eyes with poor visual recovery had even fewer VF-OCT pairings. Because of the small numbers, we trained AA on 50 ON VFs, and then tested on 25 separate ON VFs with corresponding OCTs. A larger dataset may be needed to develop ATs that are more broadly applicable. Our method of using only significant ATs to avoid random or noise contribution caused some loss in sensitivity to uncover deficits or correlations. We did not apply multiple comparison testing in our sub study as the number of ON VFs was small ($n=25$). Thus, these specific results should be regarded as preliminary and more research must be done to better understand the suggested relationship. Furthermore, although the majority of fellow eyes exhibited decomposition patterns predominantly with VF AT1, we recognize that the fellow normal eyes may not always be entirely normal. Further, prior to disease modifying therapy, individuals with ON who develop MS could potentially influence the visual field, structural features of the optic nerve, and the macula GCIPL. It is also important to note that all thickness measurements were not obtained as deviations from a normative database. We also considered un-logging TD measurements prior to running archetypal analysis to align with prior studies correlating RNFL and MD. However, the data were poor due to over- and under-emphasis of the extremes of the vision spectrum and does not account for inter-point relationships within VFs. Lastly, we lack global age-matched OCT values for normalization, unlike visual fields, as these are not currently provided by OCT manufacturers.

Future investigations will target the change in GCIPL thickness from the time of acute presentation to when recovery is complete in order to determine whether the rate or specific patterns of GCIPL thinning will correlate with residual visual field loss. Cross sectional studies report the importance of GCL thinning in patients with MS. For example, in a meta-analysis, Britze et al. demonstrated that the GCL thickness was significantly reduced in all MS patients, irrespective of previous ON status, in comparison to controls. Additionally, loss of GCL thickness was associated with reduced low contrast visual acuity and worse scores on the expanded disability status scale (EDSS)[26]. Applying AA may reveal more MS-specific subtypes of loss distinguishable from patterns due to ON.

Conclusions

Our study extended the use of AA to both 10-2 VFs and OCT, and determined patterns of retinal layer(s) thickness that correspond to patterns of VF loss. AA found that 90 days after acute ON attack, most eyes had a VF pattern at recovery that was similar to that of normal fellow eyes, even though ON eyes with recovered vision have GCIPL thinning. AA of macula GCIPL thickness was superior to a global average GCIPL thickness correlation with AT patterns of VF loss. AA suggests there may be visual processing mechanisms in the retina or in the intracranial visual pathway that compensates or preserves the function at points in the central visual field threshold in spite of retinal ganglion cell loss. The eyes with poor recovery had three meaningful patterns of VF loss and the VF weights of these eyes correlated with GCIPL thinning. This suggests that there may be a threshold of neuronal loss after which compensation mechanisms for vision improvement or preservation are not effective.

Data availability

The datasets generated and/or analyzed during the current study are not publicly available due to containing medical information but are available from the corresponding author on reasonable request.

Received: 16 April 2024; Accepted: 29 November 2024
Published online: 28 December 2024

References

1. Optic Neuritis Study Group. The 5-year risk of MS after optic neuritis. Experience of the optic neuritis treatment trial. *Neurology* **49** (5), 1404–1413 (1997).
2. Trobe, J. D., Beck, R. W., Moke, P. S. & Cleary, P. A. Contrast sensitivity and other vision tests in the optic neuritis treatment trial. *Am. J. Ophthalmol.* **121** (5), 547–553 (1996).
3. Beck, R. W. et al. A randomized, controlled trial of corticosteroids in the treatment of acute optic neuritis. The Optic Neuritis Study Group. *N Engl. J. Med.* **326** (9), 581–588 (1992).
4. De Moraes, C. G. et al. 24 – 2 visual fields miss central defects shown on 10 – 2 tests in glaucoma suspects, ocular hypertensives, and early glaucoma. *Ophthalmology* **124** (10), 1449–1456 (2017).
5. Keltner, J. L. et al. Baseline visual field profile of optic neuritis: the experience of the Optic Neuritis Treatment Trial. *Arch. Ophthalmol.* **111** (2), 231–234 (1993).
6. Klineova, S. & Kupersmith, M. Promising recovery biomarkers after first event acute demyelinating optic neuritis. *Mult Scler.* **45**, 102400 (2020).
7. Maddess, T. et al. Rapid, non-contact multifocal visual assessment in multiple sclerosis. *Neurol. Sci.* **44** (1), 273–279 (2023).
8. Costello, F. et al. Quantifying axonal loss after optic neuritis with optical coherence tomography. *Ann. Neurol.* **59** (6), 963–969 (2006).
9. Kupersmith, M. J., Anderson, S. & Kardon, R. Predictive value of 1 month retinal nerve fiber layer thinning for deficits at 6 months after acute optic neuritis. *Mult Scler.* **19** (13), 1743–1748 (2013).
10. Xu, S. C. et al. Optical coherence tomography is highly sensitive in detecting prior optic neuritis. *Neurology* **92** (6), e527–e535 (2019).
11. Hood, D. C., Anderson, S. C., Wall, M. & Kardon, R. H. Structure versus function in glaucoma: an application of a linear model. *Invest. Ophthalmol. Vis. Sci.* **48** (8), 3662–3668 (2007).
12. Hood, D. C. & Kardon, R. H. A framework for comparing structural and functional measures of glaucomatous damage. *Prog Retin Eye Res.* **26** (6), 688–710 (2007).
13. De Moraes, C. G., Sun, A. & Jarukasetphon, R. Association of Macular Visual Field measurements with Glaucoma Staging systems. *JAMA Ophthalmol.* **137** (2), 139–145 (2019).
14. Cutler, A., Breiman, L. & Archetypal Analysis *Technometrics* ;**36**(4):338–347. (1994).

15. Solli, E. et al. Archetypal analysis reveals quantifiable patterns of Visual Field loss in Optic Neuritis. *Transl Vis. Sci. Technol.* **11** (1), 27–27 (2022).
16. Li, K., Wu, X., Chen, D. Z. & Sonka, M. Optimal surface segmentation in volumetric images-a graph-theoretic approach. *IEEE Trans. Pattern Anal. Mach. Intell.* **28** (1), 119–134 (2005).
17. Garvin, M. K. et al. Automated 3-D intraretinal layer segmentation of macular spectral-domain optical coherence tomography images. *IEEE Trans. Med. Imaging*. **28** (9), 1436–1447 (2009).
18. Wang, J. K., Kardon, R. H. & Garvin, M. K. Representation and Reconstruction of Image-Based Structural Patterns of Glaucomatous Defects Using only Two Latent Variables from a Variational Autoencoder. Ophthalmic Medical Image Analysis: 8th International Workshop, OMIA 2021, Held in Conjunction with MICCAI 2021, Strasbourg, France, September 27, 2021, Proceedings 8. Springer International Publishing, (2021).
19. Raza, A. S. et al. Retinal ganglion cell layer thickness and local visual field sensitivity in glaucoma. *Arch. Ophthalmol.* **129** (12), 1529–1536 (2011).
20. Alcacer, A. Archetypes, 0.4.1. (2022).
21. Hunter, J. D. & Matplotlib A 2D Graphics Environment. *Comput. Sci. Eng.* **9** (3), 90–95 (2007).
22. Seabold, S., Perktold, J. & Statsmodels Econometric and statistical modeling with python. In *Proceedings of the 9th Python in Science Conference*. 57(61), 10-25080 (2010).
23. Hood, D. C., Anderson, S. C., Wall, M. & Kardon, R. H. Structure versus function in glaucoma: an application of a linear model. *Investig. Ophthalmol. Vis. Sci.* **48** (8), 3662–3668 (2007).
24. Demb, J. B., Haarsma, L., Freed, M. A. & Sterling, P. Functional circuitry of the retinal ganglion cell's nonlinear receptive field. *J. Neurosci.* **19** (22), 9756–9767 (1999).
25. Elze, T. et al. Patterns of functional vision loss in glaucoma determined with archetypal analysis. *J. Royal Soc. Interface*. **12** (103), 20141118 (2015).
26. Britze, J., Pihl-Jensen, G. & Frederiksen, J. L. Retinal ganglion cell analysis in multiple sclerosis and optic neuritis: a systematic review and meta-analysis. *J. Neurol.* **264**, 1837–1853 (2017).

Author contributions
DS wrote the main manuscript text and prepared figures. JW, BW, TE, MG, LP, RK, JB, MK provided feedback, edited manuscript text and figures. All authors reviewed the manuscript.

Funding
The New York Eye and Ear Infirmary Foundation, New York, N.Y.; NEI EY032522; Research to Prevent Blindness, Inc., New York, NY unrestricted grant to the Department of Ophthalmology; NEI R01 EY015473; Department of Veteran Affairs (VA) Center for the Prevention and Treatment of Visual Loss, Rehabilitation Research and Development (RR&D) I50 RX003002; VA RR&D I01RX003797.

Declarations

Competing interests
The authors declare no competing interests.

Additional information
Supplementary Information The online version contains supplementary material available at https://doi.org/10.1038/s41598-024-81835-8.

Correspondence and requests for materials should be addressed to M.J.K.